

$\vec{H} \parallel [111]$  and  $\vec{H} \parallel [011]$ . Numerical values of the ratio are also listed for some values of  $r$ . For the  $\vec{E} \perp \vec{H}$ , the table gives the ratio for the specific directions of  $\vec{E}$  used in our measurements as well as the ratio averaged over all possible directions of  $\vec{E}$ . Since the departure of  $a_e/a_i$  from unity is supposed to be responsible for the variation of absorption, Table III shows that observation (d) is to be expected,

provided that  $r = a_{11}/a_{\perp}$  is not too large. In fact, it may be expected that  $r$  is smaller than unity since  $m_{11} \gg m_{\perp}$ . The table shows that, for  $r < 1$ , a transfer of carriers to the effective valleys reduces the absorption for  $\vec{E} \parallel \vec{H}$ . This is consistent with the result that the maxima of transmission appear to correlate with passages of the Fermi level across the Landau levels in effective valleys.

<sup>†</sup>Work supported in part by U. S. Army Research Office—Durham, N. C.

<sup>\*</sup>Present address: Physics Department, Riyadh University, Riyadh, Saudi Arabia.

<sup>1</sup>R. C. Enck, A. S. Saleh, and H. Y. Fan, Phys. Rev. **182**, 790 (1969).

<sup>2</sup>B. D. McCombe, S. G. Bishop, and R. Kaplan, Phys. Rev. Letters **18**, 748 (1967).

<sup>3</sup>E. J. Johnson and D. H. Dickey, Phys. Rev. B **1**, 2676 (1970).

<sup>4</sup>A. S. Saleh, Ph.D. thesis (Purdue University, 1971) (unpublished).

<sup>5</sup>B. D. McCombe, R. J. Wagner, and G. A. Priz, Solid State Commun. **8**, 1687 (1970).

<sup>6</sup>D. L. Mitchell, E. D. Palik, and J. N. Zemel, in *Proceedings of the Seventh International Conference on the Physics of Semiconductors, Paris, 1964*, edited by J. Bok (Dunod, Paris, 1965), p. 65.

<sup>7</sup>K. F. Cuff, M. R. Ellet, C. D. Kuglin, and L. R. Williams, in *Proceedings of the Seventh International Conference on the Physics of Semiconductors, Paris, 1964*, edited by J. Bok (Dunod, Paris, 1965), p. 65.

<sup>8</sup>R. Nii, A. Kobayashi, H. Numata, and Y. Uemura,

in *Plasma Effects in Solids*, Vol. 2 of *Proceedings of the Seventh International Conference on the Physics of Semiconductors*, edited by J. Bok (Dunod, Paris, 1965), p. 65.

<sup>9</sup>M. Fujimoto, J. Phys. Soc. Japan **21**, 1706 (1966).

<sup>10</sup>W. Schilz, J. Phys. Chem. Solids **30**, 893 (1969).

<sup>11</sup>Yu. P. Ravich, B. A. Efimova, and V. I. Tamarchenko, Phys. Status Solidi **43**, 11 (1971).

<sup>12</sup>D. M. Bercha and N. V. Tarnavska, Ukr. Fiz. Zh. **9**, 642 (1964).

<sup>13</sup>R. N. Hall and J. H. Racette, J. Appl. Phys. **32**, 2078 (1961); W. Cochran, Phys. Letters **13**, 193 (1964).

<sup>14</sup>C. K. N. Patel and R. F. Slusher, Phys. Rev. **177**, 1200 (1969).

<sup>15</sup>M. S. Dresselhaus and J. G. Mavroides, Solid State Commun. **2**, 297 (1964).

<sup>16</sup>E. D. Palik and D. L. Mitchell, in *Physics of Solids in Intense Magnetic Fields*, edited by E. D. Haidemenakis (Plenum, New York, 1969), p. 90.

<sup>17</sup>R. K. Bakanas, Fiz. Tverd. Tela **12**, 3408 (1970) [Sov. Phys. Solid State **12**, 2769 (1971)].

<sup>18</sup>H. Y. Fan, in *Encyclopedia of Physics*, edited by S. Flügge (Springer, Berlin, 1967), Vol. 25/2a, p. 157.

## Tunneling in *n*-Type-GaAs-Pb Contacts under Pressure\*

P. Guétin<sup>†</sup> and G. Schröder

*Laboratoires d'Electronique et de Physique Appliquée, 94-Limeil-Brévannes, France*

(Received 15 December 1971)

The effect of hydrostatic pressure (up to 17 kbar) on the characteristics of *n*-type-GaAs-Pb tunnel contacts has been investigated both experimentally and theoretically. The shape of the background resistance  $dV/dI$  is slightly modified and its magnitude changes exponentially with pressure as a result of the barrier-height increase. In spite of some absolute discrepancies, the theory is in good qualitative agreement with the experiments. The pressure coefficient of the superconducting gap and phonon energies have been measured and compare well with other reported values. No band-structure effect has been detected.

### I. INTRODUCTION

Tunneling in solids under hydrostatic pressure has been used previously in the investigation of the tunneling process itself and of the properties of the electrodes as well. Up to now, most of the work has been devoted to *p-n* (Esaki) diodes and metal-insulator-metal (MIM) junctions. Pressure experiments on Esaki diodes have confirmed the expected exponential dependence of the tunnel current

on the energy gap.<sup>1,2</sup> Moreover, direct tunneling into the (000) valley of *n*-Ge has provided a measurement of the energy separation between the (111) and the (000) minima<sup>3</sup> of the conduction band. The energy shift of zone-edge phonons has been determined<sup>4</sup> by this technique in a few indirect-gap semiconductors which show noticeable phonon-assisted tunneling. This type of tunnel structure is well suited to pressure experiments because of its high mechanical reliability. However, only a

TABLE I. Sample characteristics.

Sample No.	Crystal	Doping density (cm <sup>-3</sup> )	Fabrication technique	Metal electrode	Experiment
C 7	epitaxial	$4.5 \times 10^{15}$ (300 °K)	IB <sup>a</sup>	Au	capacitance
CGP 7	bulk	$1.0 \times 10^{17}$ (300 °K)	VC <sup>b</sup>	Pb	capacitance
GP 26	bulk	$5.45 \times 10^{18}$ (4.2 °K)	IB	Pb	tunneling
CGP 2	bulk	$5.45 \times 10^{18}$ (4.2 °K)	VC	Pb	tunneling

<sup>a</sup>Ion-bombarded interface.<sup>b</sup>Vacuum-cleaved junction.

rather small number of materials have been used successfully and the inherent lack of knowledge of the tunnel region constitutes a major drawback. MIM structures, on the other hand, have been mainly used in the study of superconducting metals under pressure. Measurements of the energy gap of Pb,<sup>5-8</sup> Sn,<sup>9</sup> In,<sup>10</sup> Tl<sup>8,10</sup> and of the phonon spectrum of Pb<sup>6,8,11,12</sup> and Tl<sup>8</sup> have been successful up to 15 kbar. On the other hand, attempts towards observing directly the semimetal-semiconductor transition in bismuth under pressure have proved inconclusive.<sup>13</sup> If all metals or semimetals can be studied in this manner in principle, it is now clear that bringing an oxide layer about 30 Å thick up to 15 kbar without breaking through it represents more of a *tour de force* than an appealing experimental technique.

As far as we have gone, Schottky barriers present none of the above drawbacks in the sense that they are most reliable and can be made in a very clean and reproducible way with many kinds of semiconductors and counter electrodes. Cleavage in ultrahigh vacuum provides tunnel contacts which show, at room pressure at least, characteristics in close and reproducible quantitative agreement with theory.<sup>14</sup> Finally, it is worth mentioning that the essential parameters of such barriers can be conveniently determined by independent side experiments.

In this paper, we wish to present extensive results related to the behavior of *n*-GaAs-Pb contacts under hydrostatic pressure. Preliminary data have been reported elsewhere.<sup>15</sup> More emphasis is given below to experimental methods and to the comparison with theory.

## II. EXPERIMENTAL METHODS

### A. Junction Fabrication

All the junctions were made on *n*-type GaAs single crystals doped with Te. We have recently shown that junctions prepared by a slight ion bombardment (IB) method compare well to the vacuum-cleaved ones.<sup>16,17</sup> We have studied both types of junctions. The IB technique has been fully described elsewhere<sup>17</sup>: The GaAs surface is bombarded by 50-eV argon ions and is *not* annealed afterwards. Au or Pb counter electrodes are

evaporated and thin silver wires are bound to the metal dots by a small droplet of silver paste.

Vacuum-cleaved (VC) junctions are prepared in the following manner. Rectangular bars (3×10×20 mm<sup>3</sup>) are cut and the Ohmic contact is obtained by evaporating on one side a gold-tin alloy and heating it up to 200 °C. The bar is positioned between a tungsten carbide blade and an annealed copper anvil. The bakable high-vacuum system is pumped down to 5×10<sup>-10</sup> Torr and the evaporation is started. The crystal is cleaved along a (110) plane in the stream of the evaporating metal by pressing the blade on the crystal. During the metal deposition, the residual pressure is kept below 5×10<sup>-9</sup> Torr. The cleaved surface is examined under an optical microscope and several dots are selected on the smoothest surface regions. A scanning electron microscope (JEOL, JSM U3) hardly resolves the cleavage steps.

The samples, from which data under pressure are presented, are listed in Table I. Hall measurements were carried out with a clover-leaf geometry on slices adjacent to the tunnel or capacitance samples. The doping levels indicated in Table I refer to the temperature at which the pressure experiments were done. All tunnel junctions have been made with lead so that superconductivity could be used as a test for tunneling behavior.

### B. Sample Holders

The experiments under hydrostatic pressure have been carried out at the Faculté des Sciences d'Orsay. A complete description of the apparatus can be found elsewhere.<sup>18</sup> We use a high-pressure bomb filled with isopentane as a transmitting fluid. The samples are positioned onto an obturator equipped with seven electrical feedthroughs. The bomb is connected through a capillary tube to the main press where the pressure is measured with a manganin gauge. Before putting the bomb into the cryostat, a full cycle between 0 and 17 kbar is performed at room temperature in order to test the behavior of the selected junctions. As the bomb cools down, the isopentane freezes at a temperature which depends on pressure (approximately 145 °K at 3 kbar and 260 °K at 16 kbar). In order to control the pressure *P* during this operation, the

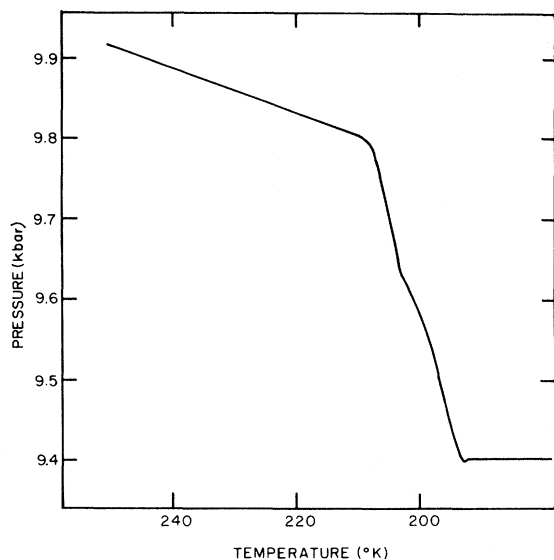


FIG. 1. Variation of pressure during the freezing of the transmitting fluid. Deviation from a sharp pressure drop is due to the temperature gradient along the bomb.

cooling is started slowly from the bottom of the bomb by a liquid-nitrogen circulation. At the same time, the head of the bomb is heated with an electrical coil. This procedure keeps the communication between the bomb and the press and allows a continuous measure of  $P$  versus temperature (Fig. 1). A pressure drop of about 600 bar results from the freezing of the fluid, and therefore creates a slight gradient inside the bomb. The value of the pressure on the sample is chosen as the value at the middle of the drop  $\pm 300$  bar. The slight pressure variation which may occur when temperature goes down from the freezing point to 4.2 °K is neglected. No magnetic field was available in the present experiments.

### C. Measuring System

The barrier heights are measured by the differential capacitance method with a 75-A-S8 Boonton bridge. The ac tunneling resistances  $dV/dI$  and  $d^2I/dV^2$  are plotted with a classical system.<sup>19</sup> The differential resistances of the junctions range from 20 to 1000  $\Omega$  according to the pressure. In order to obtain an accurate determination of the phonon energies, the  $X$  channel of the  $XY$  recorder is systematically calibrated with a digital voltmeter before each measurement. All the energies reported in the text are corrected at all pressures for the half-gap value  $\Delta$  of the superconducting counter electrode. Throughout this work,  $V > 0$  corresponds to electron injection from the semiconductor into the metal.

### D. Reproducibility

We have already reported<sup>14</sup> that, generally speaking, the reproducibility of vacuum-cleaved tunnel contacts is excellent regarding the absolute resistance, the background shape, and the position of the resistance maximum. Since changing the pressure actually requires warming up the transmitting fluid, junctions are subjected to many pressure and temperature cycles. They prove mechanically very reliable in the sense that very few junctions have shown signs of deterioration even at the highest pressure (17 kbar). Tunneling characteristics at  $P=0$  are systematically measured before and after the experiments: The background shape and lead gap undergo only minor irreversible changes (typical variation of  $\Delta$  is 2%). The position of the phonon structure does not vary appreciably (1%). However, the low-temperature value of the zero-bias resistance tends to increase by a factor of 2–4. This resistance increase may be due to a change in the interface conditions. Indeed, it is not surprising that the Pb-GaAs intimate contact is modified by the severe experimental conditions.

### III. BARRIER HEIGHT

The barrier height  $V_B$  of metallic contacts cleaved and ion-bombarded GaAs has been determined by the capacitive method at 300 and 77 °K for  $P=0$ <sup>14,17</sup> and at 300 °K for various pressures. Figure 2 shows a typical plot of  $1/C^2$  versus applied voltage. The intercept  $V_0$  of the curves with the  $X$  axis shifts towards higher voltage when pressure goes up, indicating an increase of  $V_B$ . The curves remain linear and a careful analysis leads to a

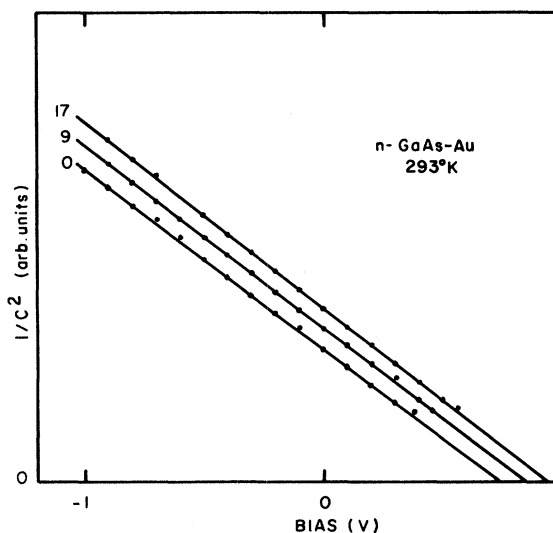


FIG. 2. Capacitance-voltage dependence of sample C 7 at 0, 9, and 17 kbar.

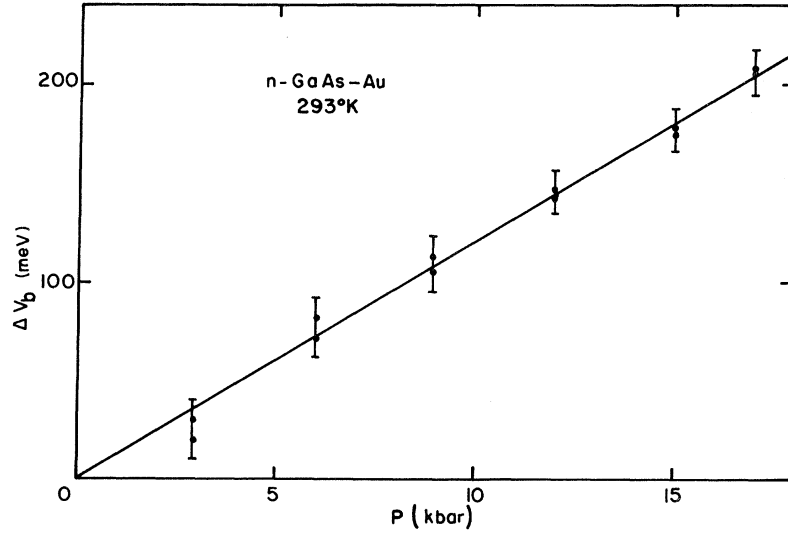


FIG. 3. Variation of the barrier height with applied pressure for two junctions of sample C 7.

small variation of the slope  $\delta s/s \approx 3\%$  between 0 and 17 kbar.  $s$  depends on the carrier density  $N$ , the area of the junction  $A$ , and the dielectric constant  $\epsilon$ , which hardly vary under pressure. From  $\delta s/s$  and the bulk modulus<sup>20</sup> we estimate that  $d\epsilon/\epsilon \approx -2\%$  between 0 and 17 kbar. This result may be compared to the variation of  $\epsilon$  in germanium:  $(d\epsilon/dP)/\epsilon = -1.2 \times 10^{-3} \text{ kbar}^{-1}$ .

When the semiconductor is nondegenerate,  $V_B$  is given by<sup>21</sup>

$$V_B = V_0 + \mu_F + kT/e, \quad (1)$$

where  $\mu_F$  is the Fermi level below the bottom of the conduction band and  $T$  the temperature of the junction. We can estimate the pressure dependence of  $\mu_F$  which is calculated from

$$N = 2 \left( \frac{2\pi m^* kT}{h^2} \right)^{3/2} e^{-\mu_F/kT}, \quad (2)$$

where all symbols have their usual meaning. Thus, for constant  $N$ ,

$$\delta \mu_F = \frac{3}{2} kT (\delta m^*/m^*) \quad (3)$$

The variation of  $m^*$  is approximately given by<sup>22</sup>

$$m^*(P)/m^*(0) = E_G(P)/E_G(0), \quad (4)$$

where

$$E_G(P) = E_G(0) + \alpha P \quad (5)$$

is the pressure-dependent energy gap. Equations (3)–(5) lead to

$$\delta \mu_F = 3kT\alpha P/2E_G(0). \quad (6)$$

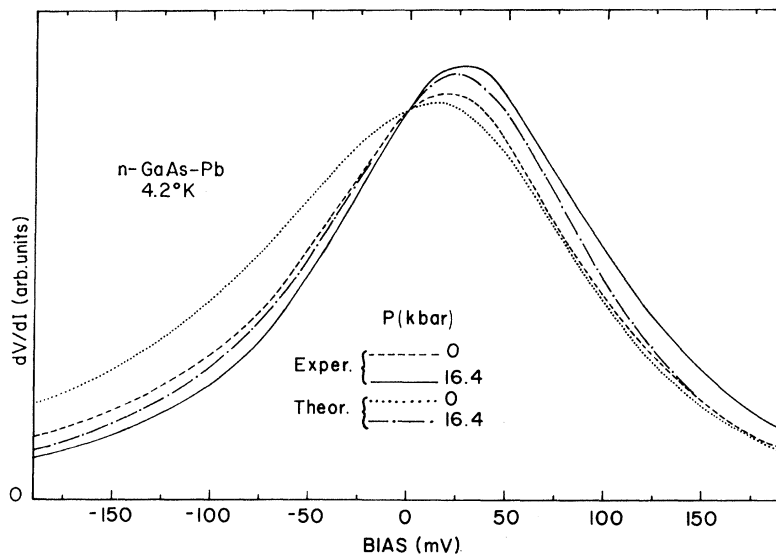


FIG. 4. Experimental and theoretical variations of  $dV/dI$  versus bias voltage for  $P=0$  and 16.4 kbar (IB sample GP 26). The superconducting structures around zero bias have been omitted for clarity.

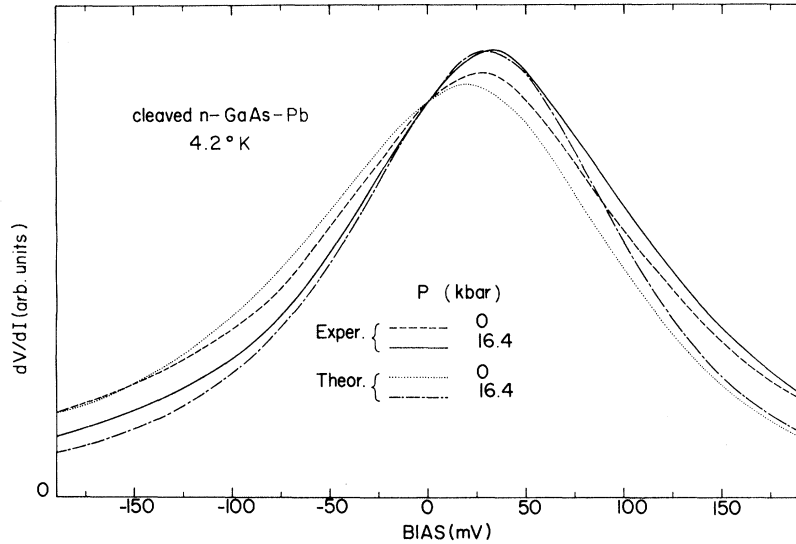


FIG. 5. Experimental and theoretical variations of  $dV/dI$  versus bias voltage for 0 and 16.4 kbar (VC sample CGP 2). The superconducting structures around zero bias have been omitted for clarity.

Using the parameters listed in Sec. III, we deduce that  $\delta\mu_F \approx 5$  meV at 17 kbar. The pressure dependence of  $V_B$  is plotted in Fig. 3 for two diodes of sample C 7. The slope  $\partial V_B/\partial P$  is equal to  $12 \pm 0.5$  meV/kbar, and with sample CGP 7 we measured  $10.9 \pm 0.7$  meV/kbar.  $\partial V_B/\partial P$  appears to be quite independent of the metal electrode and of the doping density. These results are in good agreement with the experimental determinations<sup>23</sup> of  $\alpha$  (between 10.6 and 12 meV/kbar), which means that the Fermi level at the interface remains pinned with respect to the valence band when pressure goes up. This is analogous to what happens when the temperature is lowered<sup>24</sup> and confirms the role played by "surface states" in determining the potential barrier.

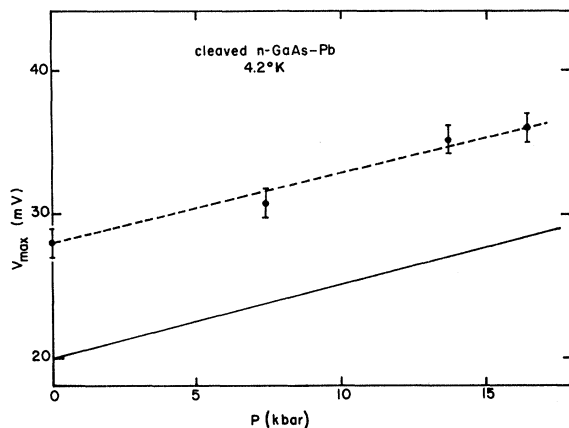


FIG. 6. Pressure dependence of  $V_{\max}$ . Dashed line: experimental result; full line: theoretical calculation (see Sec. IV B).

#### IV. BACKGROUND RESISTANCE

##### A. Experimental Results

Typical  $dV/dI$  data obtained from IB and VC junctions are shown in Figs. 4 and 5. Included for comparison are the corresponding theoretical curves (see Sec. IV B). All resistances have been normalized at  $V=0$ . It is clear that the over-all shape of  $dV/dI$  does not experience a strong modification. On both types of junctions, the main effect can be pictured as an over-all shift of the curve towards forward bias as a consequence of the increase of the barrier height.<sup>14</sup> Although the position of the resistance maximum  $V_{\max}$  is not

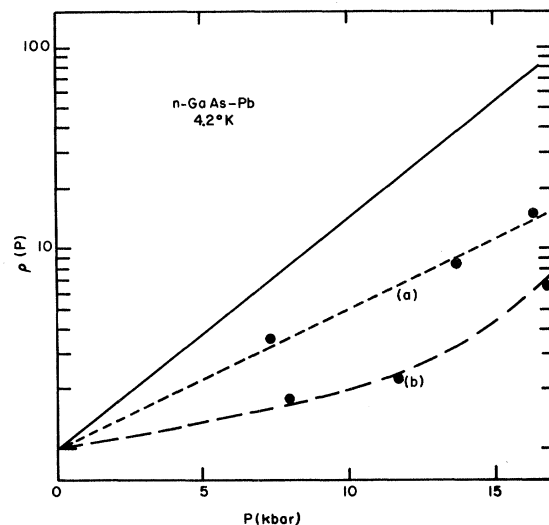


FIG. 7. Pressure dependence of  $\rho(P) = R_0(P)/R_0(0)$ . Short-dashed line: VC sample; long-dashed line: IB sample; full line: theory (see Sec. IV B).

TABLE II. Parameters for GaAs used in the numerical calculation.

Relative static dielectric constant	$\epsilon = 12.5$
Effective mass	$m^* = 0.07m$
Energy gap at 0°K and $P=0^a$	$E_G(0) = 1.522 \text{ eV}$
Pressure coefficient of $E_G$	$\alpha = 12 \text{ meV/kbar}$
Barrier heights for $P=0^b$	$V_B = 0.83 \text{ eV (IB)}$ $V_B = 0.92 \text{ eV (VC)}$
Pressure coefficient of $V_B$	$\partial V_B / \partial P = 12 \text{ meV/kbar}$
Fermi degeneracy at zero pressure	$\mu_F = 150 \text{ meV}$

<sup>a</sup>M. D. Sturge, Phys. Rev. 127, 768 (1962).

<sup>b</sup>References 14 and 17.

identical for the IB and VC contacts, the shift  $\Delta V_{\text{max}} \approx 8 \text{ mV}$  between 0 and 16.4 kbar is the same. Figure 6 shows that the pressure dependence of  $V_{\text{max}}$  is linear with  $P$ , i. e., with  $V_B$ . Owing to the barrier-height variation, one can expect an increase of the absolute resistance of the junctions. This can be illustrated by the zero-bias value  $R_0(P)$  of  $dV/dI$ . Typical values for a junction of  $0.33 \text{ mm}^2$  studied on sample CGP 2 are  $R_0(0) = 12 \Omega$  and  $R_0(P) = 180 \Omega$  at  $P = 16.4 \text{ kbar}$ . In Fig. 7, a plot of  $\rho(P) = R_0(P)/R_0(0)$  for both types of junctions shows that  $\rho(P)$  for VC junctions increases nearly exponentially with  $P$ . On the other hand, the pressure dependence of  $\rho$  in the case of IB contacts is not as fast and not exponential.

### B. Comparison with Theory and Discussion

We assume a homogeneous semiconductor and a perfect interface with specular transmission between both materials. The differential resistance is computed in a pure WKB approximation<sup>14</sup> (no extra prefactor) with a parabolic barrier and the Franz two-band model.<sup>25</sup> The quadrature over the momentum parallel to the interface is carried out and the computation is done with the parameters listed in Table II. We neglect the pressure dependence of  $\epsilon$ ,  $N$ , and  $A$ . Variations of  $m^*$  and  $E_G$  with  $P$  are given by (4) and (5). The Fermi degeneracy  $\mu_F$  has been calculated for a nonparabolic conduction band and is given by

$$N = \frac{1}{3\pi^2} \left( \frac{2m^*}{\hbar^2} \right)^{3/2} \left( \frac{(1 - m^*/m)^2}{E_G} \mu_F^2 + \mu_F \right)^{3/2}. \quad (7)$$

The theoretical curves of  $dV/dI$  plotted in Figs. 4 and 5 show the same kind of over-all shift towards forward bias as the experimental curves do. Figure 6 shows that the experimental increase of  $V_{\text{max}}$  agrees with theory, although a systematic discrepancy exists in the absolute values. This kind of disagreement has already been observed and discussed.<sup>14</sup> It is worth mentioning here that the semiconductor energy gap has a non-negligible influence

on the resistance characteristics. This is the consequence of the coupling of conduction- and valence-band states. The calculation predicts that the change of  $V_B$  alone would increase  $V_{\text{max}}$  by 15 mV at 16 kbar. Since it can be shown that the variation of  $m^*$  and the related decrease of  $\mu_F$  (about 20 meV) at the same pressure tend also to increase  $V_{\text{max}}$ , we conclude that the increase of  $E_G$  alone tends to reduce  $V_{\text{max}}$  and limits the net shift to 8 meV. In previous experiments,<sup>14</sup> the influence of  $V_B$  and  $N$  on the background shape was studied by varying the metal electrode or the doping density of GaAs. The present results show that pressure offers a unique way to vary  $E_G$  and to observe again the fairly good agreement between theory and experiment.

The theoretical variation of  $\rho(P)$  is shown in Fig. 7. As predicted from an approximate calculation,<sup>26</sup>  $R_0(0)$  (equal to  $7 \Omega$  for  $0.33 \text{ mm}^2$ ) increases with  $V_B$  following

$$R_0(0) \approx B e^{V_B/E_0}, \quad (8)$$

where

$$E_0 = (e^2 N \hbar^2 / 4m^* \epsilon)^{1/2}. \quad (9)$$

The exponential factor contains all the parameters which have a drastic effect on the magnitude of  $R_0$ :  $N$ ,  $m^*$ , and  $V_B$ . The variation of  $E_0$  with pressure can be neglected, since  $E_0 = 44 \text{ meV}$  for  $P = 0$  and  $41.5 \text{ meV}$  for  $16.4 \text{ kbar}$ . Let us assume that  $B$ , which contains the influence of  $E_G$  on  $R_0(0)$ , is constant with pressure; then

$$\rho(P) = e^{\Delta V_B/E_0}. \quad (10)$$

For 16.4 kbar,  $\Delta V_B = 197 \text{ meV}$ . Taking a mean value for  $E_0$  (43 meV), we find  $\rho(P) = 95$  instead of 85 obtained by the full computation. Thus, expression (8) constitutes a good approximation and reveals that the essential cause of the resistance increase with  $P$  is the variation of the barrier height. It is interesting to note that the variation of  $E_G$ , which affects the dispersion relation inside the energy gap and is of some importance in the determination of  $V_{\text{max}}$ , has only a minor effect on  $R_0$ . Figure 7 clearly shows that the calculation overestimates the variation of  $R_0(P)$ . Even though the barrier-height increase with pressure has been measured at  $300^\circ \text{K}$  only, it is unlikely that  $\partial V_B / \partial P$  would depend so much on  $T$  to allow a good fit of the curves at low temperature. It is more likely that some effect neglected in the simple model becomes important at high pressure when the direct transmission coefficient decreases. A comparison between the two experimental curves in Fig. 7 suggests a strong influence of the interface. Whether a breakdown of the  $k$  parallel conservation law owing to IB-induced defects or locally rough interfaces on VC junctions could explain this disagree-

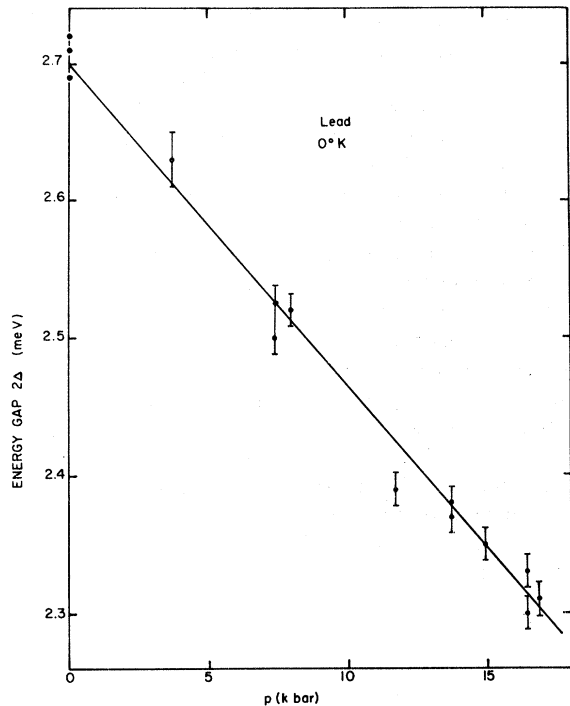


FIG. 8. Pressure dependence of the lead energy gap.

ment is unclear at present.

#### C. Band-Structure Effects

The onset of tunneling into a higher band has been observed in *n*-Ge.<sup>27</sup> The related decrease of

the resistance is expected to be noticeable only if the transmission coefficient for this new tunneling path is comparable to the one which corresponds to the lower band. In GaAs, the energy gap  $\Delta E$  between the (100) upper valleys and the (000) minimum responsible of the main current is about 0.37 eV at 4.2 °K and  $P=0$ . The conductivity effective mass has been estimated<sup>28</sup> at  $m^*(000)=0.41m$ . Under application of pressure,  $\Delta E$  decreases at the rate of<sup>29</sup>  $-13.5 \times 10^{-6}$  eV/kbar and is reduced to 140 meV at 17 kbar. For the same value of  $P$ ,  $\mu_F$  is equal to 130 meV. We could expect that an additional current, if any, might manifest itself around  $-10$  mV at reverse bias. A careful analysis of our experimental data has failed to show any evidence of tunneling in the higher valleys and therefore confirms the theoretical prediction that the larger barrier height and effective mass result in a much too low transmission probability.

#### V. LO PHONON OF GaAs

The spectroscopic aspect of the tunneling experiments has been investigated to study the variation of the superconducting gap (Fig. 8) and of the TA and LA phonon energies of lead (Fig. 9).  $2\Delta$  is found to vary linearly from 2.7 meV at  $P=0$  to 2.3 meV at 17 kbar. The logarithmic variations of the two phonon energies are approximately the same and numerical results have been summarized in a table published elsewhere.<sup>15</sup>

An approximately antisymmetric structure in the resistance  $dV/dI$  of metal-GaAs tunnel junctions has been observed for biases  $eV \approx \pm \hbar\omega_0$ , the

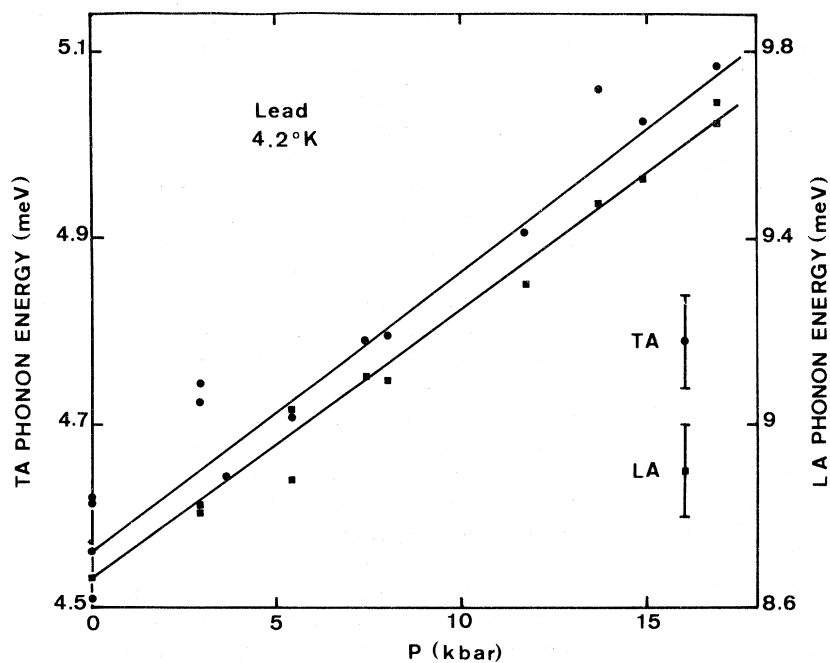


FIG. 9. Pressure dependence of the TA and LA phonon energies of lead.

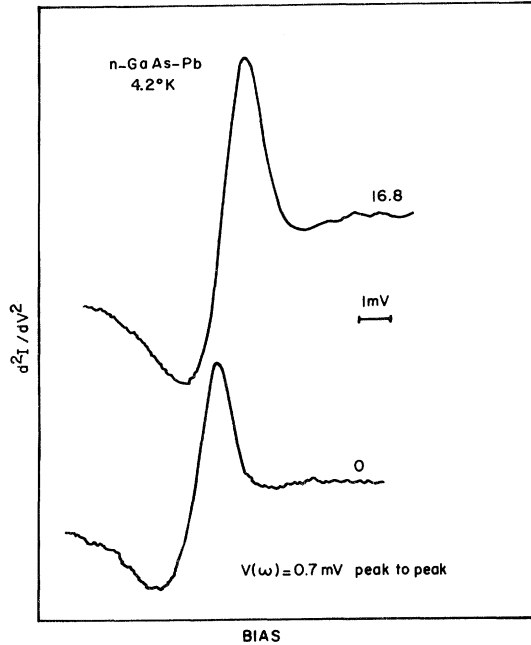


FIG. 10.  $d^2I/dV^2$  at forward bias showing the shift of the LO(000) structure when  $P$  increases from 0 to 16.8 kbar. Pb is in the superconducting state.

energy of the  $k \sim 0$  optical phonon in GaAs.<sup>16,25,30,31</sup> This structure has been interpreted in terms of self-energy effects in the semiconductor electrode.<sup>32</sup> For direct bias, the line shape of the  $d^2I/dV^2$ -vs- $V$  curve, shown in Fig. 10, consists of a dip and a peak located at  $4.2^\circ\text{K}$  at  $34.55 \pm 0.1$  and  $36.35 \pm 0.1$  meV, respectively. Experimental values of the LO(000) phonon energy between 36.5 and 36.8 meV for pure bulk GaAs at the same temperature have been obtained from infrared reflection,<sup>33</sup> Raman spectroscopy,<sup>34</sup> and optical transmission.<sup>35</sup> Therefore, we may assume that the position of the peak gives a direct measurement of the pressure coefficient of the LO(000) phonon. This method seems consistent, since the line shape at  $V > 0$  is not modified by pressure. We have plotted in Fig. 11(a) the peak energy corrected for the lead gap. The GaAs LO phonon energy varies linearly with pressure at  $(6.8 \pm 0.5) \times 10^{-5}$  meV/bar. The structure at reverse bias is not as sharp and has not been considered for this determination. The individual Grüneisen parameter  $\gamma_0(\text{LO}) = (B/\omega_0) \times (\partial\omega_0/\partial P)_T$  is calculated with the bulk modulus  $B = 0.747 \times 10^3$  (in kbar). We find  $\gamma_0(\text{LO}) = 1.4 \pm 0.1$ . Previous determinations of  $\gamma_0$  have been reported by Mitra *et al.*<sup>36</sup> for some compounds belonging to the zinc-blende structure family. These measurements led to three conclusions: (i) The value of  $\gamma_0(\text{LO}) \approx 1$  is approximately the same for all compounds investigated, (ii)  $\gamma_0(\text{TO}) > \gamma_0(\text{LO})$ , and (iii) the ratio  $\gamma_0(\text{TO})/\gamma_0(\text{LO})$  increases with ionicity de-

finied as the effective charge per valence electron. Our results do not follow closely conclusion (i). The plot<sup>38</sup> of  $\gamma_0(\text{TO})$  vs the effective charge  $e^*$  provides an estimate of the Grüneisen parameter for the TO(000) phonon in GaAs:  $\gamma_0(\text{TO}) \approx 1.32$ , which is in much better agreement with our experimental value. The TO phonon might be involved in the tunnel structure, but in absence of a clear understanding of the line shape, we cannot draw any firm conclusion.

The intensity of the LO phonon structure measured by  $R\Delta i''$ , where  $R$  is the resistance of the junction and  $\Delta i''$  the amplitude of the down and up structure, increases under pressure. The relative variation of its intensity  $Y$  is shown in Fig. 11. It reaches about 20% at 15 kbar. This enhancement may be due to a change of the electron-phonon coupling or, more simply, to the barrier deformation under pressure.

## VI. CONCLUSION

These experiments have shown that metal-semiconductor tunnel contacts can be successfully studied under high hydrostatic pressure and that their behavior is reasonably well accounted for in the frame of the usual tunneling model. They constitute a convenient and reliable tool, which has been used in the particularly simple case of  $n$ -GaAs. The relatively small and smooth changes of the tunnel characteristics are due to the fact that, for all applied pressures, the conduction band remained centered at  $k=0$  and isotropic. This result and the absence of zero-bias anomaly in contacts made by the VC technique show that  $n$ -GaAs is well suited to the study of specific changes of the counter electrode properties such as superconductivity and semimetal-semiconductor transition. In the latter example, the opening of a forbidden gap should manifest itself as a zero-bias resistance peak which could be extracted from the background resistance without difficulty. The results obtained on the superconductivity of lead compare well with the data obtained with MIM junctions and the technique could be easily extended to all superconducting metals. In view of such a study it is worth pointing out that the IB technique is appropriate since we have shown that (i) a slight bombardment does not affect the properties of the counter electrode, (ii) the experimental setup is simpler than the VC technique apparatus, and (iii) we can get rid of zero-bias anomalies.

On the semiconductor side, many materials other than GaAs present interesting band-structure effects in the range of pressure presently available. Along this line, we have undertaken experiments<sup>37</sup> in  $n$ -GaSb for which a band crossing occurs around 10 kbar which strongly affects the conductance

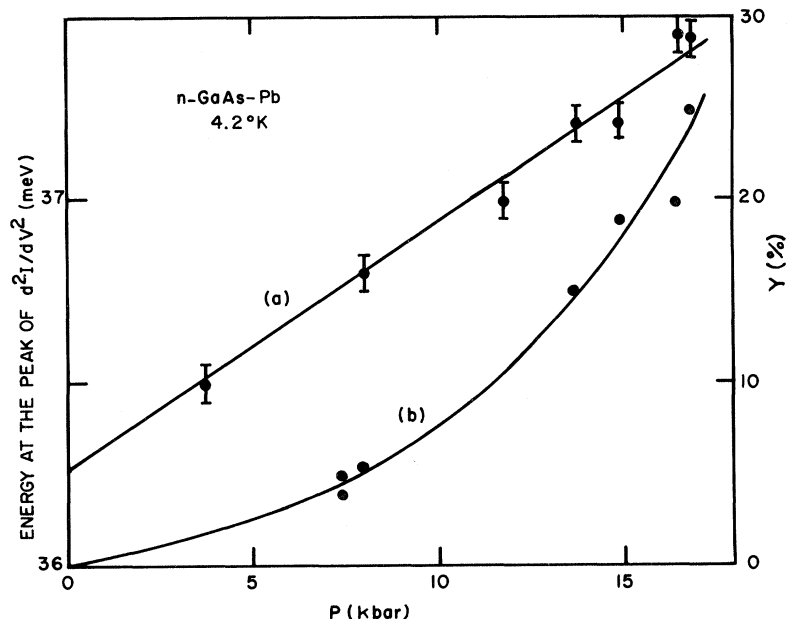


FIG. 11. Pressure dependence of the zone-center optical phonon energy of GaAs (a) and of its relative amplitude (b).

background and correspondingly the many-body effects.

#### ACKNOWLEDGMENTS

We wish to thank D. Jerome for making available

the high-pressure apparatus of Orsay and Professor E. Guyon for his constant interest in this work. R. Duchesne and M. Nelson-Pautier are gratefully acknowledged for their skillful technical help.

\*This work is supported by the Délégation Générale à la Recherche Scientifique et Technique.

†Based partially on a Doctorat d'Etat ès Sciences Physiques to be presented at the Faculté des Sciences d'Orsay, 1972.

<sup>1</sup>S. L. Miller, M. I. Nathan, and A. C. Smith, *Phys. Rev. Letters* **4**, 60 (1960).

<sup>2</sup>M. I. Nathan and W. Paul, in *Proceedings of the International Conference on Semiconductor Physics, Prague, 1960* (Czechoslovakian Academy of Sciences, Prague, 1961), p. 209.

<sup>3</sup>H. Fritzsche and J. J. Tiemann, *Phys. Rev.* **130**, 617 (1963).

<sup>4</sup>H. Fritzsche, in *Tunneling Phenomena in Solids*, edited by E. Burstein and S. Lundqvist (Plenum, New York, 1969), p. 167.

<sup>5</sup>A. A. Galkin and V. M. Svistunov, *Phys. Status Solidi* **26**, K55 (1968).

<sup>6</sup>J. P. Franck and W. J. Keeler, *Phys. Rev. Letters* **20**, 379 (1968).

<sup>7</sup>N. V. Zavaritskii, E. S. Itskevitch, and A. N. Voronovskii, *Zh. Eksperim. i Teor. Fiz. Pis'ma v Redaktsiyu* **7**, 271 (1968) [*JETP Letters* **7**, 211 (1968)].

<sup>8</sup>A. A. Galkin, V. M. Svistunov, A. P. Dikii, and V. N. Taranenko, *Zh. Eksperim. i Teor. Fiz.* **59**, 77 (1970) [*Sov. Phys. JETP* **32**, 44 (1971)].

<sup>9</sup>A. A. Galkin, A. P. Dikii, and V. M. Svistunov, *Phys. Status Solidi* **30**, K107 (1968).

<sup>10</sup>A. A. Galkin, V. M. Svistunov, and A. P. Dikii, *Phys. Status Solidi* **35**, 421 (1969).

<sup>11</sup>J. P. Franck and W. J. Keeler, *Phys. Letters* **25A**, 624 (1967).

<sup>12</sup>J. P. Franck, W. J. Keeler, and T. M. Wu, *Solid State Commun.* **7**, 483 (1969).

<sup>13</sup>J. R. Vainsys, D. B. McWhan, and J. M. Rowell, *J. Appl. Phys.* **40**, 2623 (1969).

<sup>14</sup>P. Guétin and G. Schröder, *J. Appl. Phys.* **42**, 5689 (1971).

<sup>15</sup>P. Guétin and G. Schröder, *Solid State Commun.* **9**, 591 (1971).

<sup>16</sup>P. Guétin and G. Schröder, *Solid State Commun.* **8**, 291 (1970).

<sup>17</sup>P. Guétin and G. Schröder, *J. Appl. Phys.* **43**, 549 (1972).

<sup>18</sup>G. Malfait and D. Jerome, *Rev. Phys. Appl.* **4**, 467 (1969).

<sup>19</sup>D. E. Thomas and J. M. Rowell, *Rev. Sci. Instr.* **36**, 1301 (1965).

<sup>20</sup>H. J. McSkimin, A. Jayaraman, and P. Andreatch, *J. Appl. Phys.* **38**, 2362 (1967).

<sup>21</sup>A. Goodman, *J. Appl. Phys.* **34**, 329 (1963).

<sup>22</sup>H. Ehrenreich, *Phys. Rev.* **120**, 1951 (1960).

<sup>23</sup>R. Bendorius and A. Shileika, *Solid State Commun.* **8**, 1111 (1970).

<sup>24</sup>C. A. Mead and W. G. Spitzer, *Phys. Rev. Letters* **10**, 471 (1963).

<sup>25</sup>J. W. Conley and G. D. Mahan, *Phys. Rev.* **161**, 681 (1967).

<sup>26</sup>R. Stratton and F. A. Padovani, *Solid State Electron.* **10**, 813 (1967).

<sup>27</sup>J. W. Conley and J. J. Tiemann, *J. Appl. Phys.* **38**, 2880 (1967).

<sup>28</sup>G. D. Pitt and J. Lees, *Phys. Rev. B* **2**, 4144 (1970).

<sup>29</sup>R. W. Keyes, in *Semiconductors and Semimetals*,

edited by R. K. Williardson and A. C. Beer (Academic, New York, 1968), Vol. IV, p. 327.

<sup>30</sup>D. C. Tsui, Phys. Rev. Letters 21, 994 (1968).

<sup>31</sup>M. Mikkor and W. C. Vassell, Phys. Rev. B 2, 1875 (1970).

<sup>32</sup>C. B. Duke, *Tunneling in Solids* (Academic, New York, 1969), Chaps. VI and VII.

<sup>33</sup>M. Hass and B. W. Henvis, J. Phys. Chem. Solids 23, 1099 (1962).

<sup>34</sup>A. Mooradian and G. B. Wright, Solid State Commun. 4, 431 (1966).

<sup>35</sup>S. Iwasa, I. Balslev, and E. Burstein, in *Proceedings of the International Conference on Semiconductor Physics, Paris, 1964* (Dunod, Paris, 1964), p. 1077.

<sup>36</sup>S. S. Mitra, O. Brafman, W. B. Daniels, and R. K. Crawford, Phys. Rev. 186, 942 (1969).

<sup>37</sup>P. Guétin and G. Schröder, Phys. Rev. Letters 27, 326 (1971).

PHYSICAL REVIEW B

VOLUME 5, NUMBER 10

15 MAY 1972

## Electron-Paramagnetic-Resonance Detection of Optically Induced Divacancy Alignment in Silicon

C. A. J. Ammerlaan

*Natuurkundig Laboratorium, Universiteit van Amsterdam, Amsterdam, The Netherlands*

and

G. D. Watkins

*General Electric Corporate Research and Development, P. O. Box 8, Schenectady, New York 12301*

(Received 11 January 1972)

An EPR study was made of the divacancy in silicon, produced by 1.5-MeV electron irradiation at room temperature, under illumination with polarized light. A light-induced alignment of divacancies among the various Jahn-Teller distortion directions in the lattice is observed for the singly positively charged state, as monitored directly in the corresponding EPR spectrum. Optical bands at 1.8 and 3.9  $\mu$ , which have been previously correlated with the positive divacancy, are found to have no alignment effect. Instead a band at  $\sim 2.15 \mu$ , not previously reported, is found to have the maximum alignment efficiency. The transition-dipole-moment direction for this band is determined with respect to the defect axes.

### I. DIVACANCY PROPERTIES

The divacancy  $V_2$  in irradiated silicon has been extensively investigated by electron paramagnetic resonance,<sup>1-4</sup> infrared absorption,<sup>5-10</sup> and photoconductivity.<sup>10-13</sup> From the EPR experiments it was deduced that there are four equivalent atomic orientations for the divacancy, corresponding to the four  $\langle 111 \rangle$  nearest-neighbor vacancy-vacancy directions in the silicon lattice. Each of these exists in one of three different electronic configurations, which are linked with small Jahn-Teller distortions of the lattice surrounding the divacancy. The defect has the symmetry of the point group  $2/m(C_{2h})$ . A model of the divacancy consistent with the results of EPR studies is shown in Fig. 1. One-electron molecular-orbital wave functions, obtained by linear combination of atomic orbitals (LCAO), and the corresponding energy levels are given in Fig. 2. The divacancy is a paramagnetic center for both the singly positively and the singly negatively charged states. The former state occurs for a Fermi level below  $E_v + 0.25$  eV. In this charge state there is only one electron in the  $b + b' - \lambda_1(a + d + a' + d')$  bonding orbital. The corresponding EPR spectrum is named<sup>3</sup> G6.

Three optical absorption bands in the infrared, at 1.8, 3.3, and 3.9  $\mu$ , respectively, have been attributed to the divacancy.<sup>7</sup> This correlation is mainly based on the explanation by the divacancy model of the response of these bands to uniaxial stress, and on the annealing properties. The absorption bands are only observable for restricted ranges of the Fermi level within the gap, i. e., for certain charge states of the divacancy. From these arguments Cheng *et al.*<sup>7</sup> originally concluded that the 3.3- $\mu$  band arises from  $V_2^{2-}$ , the 3.9- $\mu$  band from  $V_2^+$ , and the 1.8- $\mu$  band from  $V_2^+$ ,  $V_2^0$ , and  $V_2^-$ . The allowed electric dipole transitions are indicated in the LCAO energy-level scheme depicted in Fig. 2. For all three bands the transition dipole moments were deduced to lie in the XY plane. The 1.8- $\mu$  band was tentatively identified as the transition labeled  $\alpha$ . In subsequent work Cheng and Vajda<sup>9</sup> used polarized light and observed a light-induced dichroism of the 1.8- and 3.3- $\mu$  bands. The kinetics of the recovery were studied for each band and it was found that neither could be directly correlated with the Jahn-Teller reorientation kinetics previously studied in uniaxial stress studies for the EPR observable states  $V_2^+$  and  $V_2^-$ . Although this remains consistent with the identification of